Experimental Quantum Error Correction

Raymond Laflamme

Institute for Quantum Computing, Waterloo

laflamme@iqc.ca

www.iqc.ca

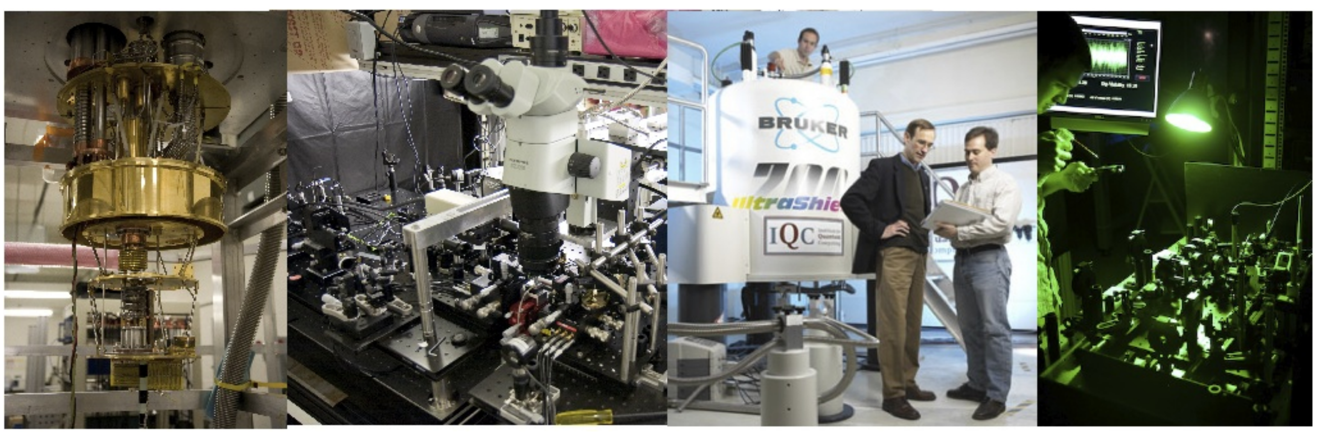

QEC11, December 2011

Plan

- **Introduction**
- **Benchmarking and certifying gates**
- **Implementations of QEC**
- **Conclusion**

Threshold theorem

A quantum computation can be as long as required with any desired accuracy as long as the noise level is below a threshold value

$P < 10^{-6,-5,-4,\ldots,-1?}$

See Andrew Landahl's talk

Knill et al.; Science, 279, 342, 1998

Kitaev, Russ. Math Survey 1997

Aharonov & Ben Or, ACM press

Preskill, PRSL, 454, 257, 1998

...

Significance:

-imperfections and imprecisions are not fundamental objections to quantum computation

-it gives criteria for scalability

-its requirements are a guide for experimentalists

-it is a benchmark to compare different technologies

Threshold theorem

Accuracy threshold

Theorem proved...
what is left?
-what is the value of the threshold?
-what is the operational cost?

A quantum computation can be as long as required with any desired accuracy as long as the noise level is below a threshold value

$P < 10^{-6,-5,-4,...,-1?}$

See Andrew Landahl's talk

Knill et al.; Science, 279, 342, 1998

Kitaev, Russ. Math Survey 1997

Aharonov & Ben Or, ACM press

Preskill, PRSL, 454, 257, 1998

...

Significance:

-imperfections and imprecisions are not fundamental objections to quantum computation

-it gives criteria for scalability

-its requirements are a guide for experimentalists

-it is a benchmark to compare different technologies

Ingredients for FTQEC

- **Parallel operations**
- **Good quantum control**
- **Ability to extract entropy**
- **Knowledge of the noise**
  - **No lost of qubits**
  - **Independent or quasi independent errors**
  - **Depolarising model**
  - **Memory and gate errors**
  - **...**

Ingredients for FTQEC

- **Parallel operations**
- **Good quantum control**
- **Ability to extract entropy**
- **Knowledge of the noise**
  - No lost of qubits
  - Independent or quasi independent errors
  - Depolarising model
  - Memory and gate errors
  - ...

and lots of qubits...

Progress in experimental QIP

- **# of qubits vs time**

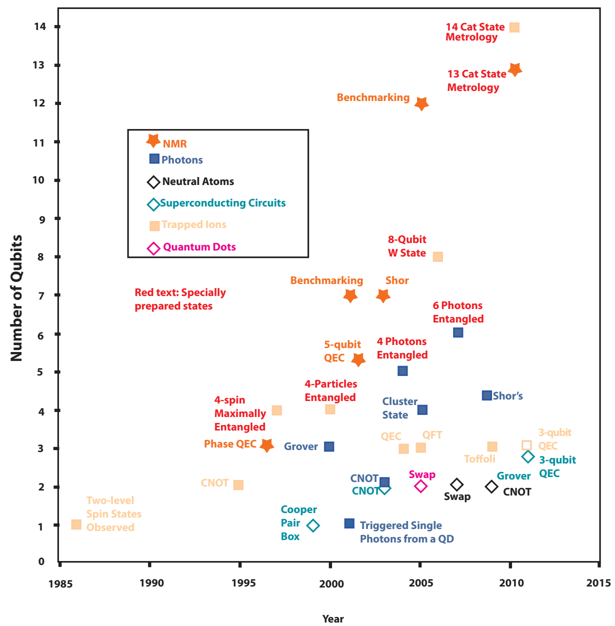

Adapted from Michael Mandelberg

- **Increasing control of qubits**

Table 1 | Current performance of various qubits

Type of qubit	T_2	Benchmarking (%)		References
		One qubit	Two qubits	
Infrared photon	0.1 ms	0.016	1	20
Trapped ion	15 s	0.48†	0.7*	104–106
Trapped neutral atom	3 s	5		107
Liquid molecule nuclear spins	2 s	0.01†	0.47†	108
e^- spin in GaAs quantum dot	3 μs	5		43, 57
e^- spins bound to ^{31}P:^{28}Si	0.6 s	5		49
^{29}Si nuclear spins in ^{28}Si	25 s	5		50
NV centre in diamond	2 ms	2	5	60, 61, 65
Superconducting circuit	4 μs	0.7†	10*	73, 79, 81, 109

Measured T_2 times are shown, except for photons where T_2 is replaced by twice the hold-time (comparable to T_1) of a telecommunication-wavelength photon in fibre. Benchmarking values show approximate error rates for single or multi-qubit gates. Values marked with asterisks are found by quantum process or state tomography, and give the departure of the fidelity from 100%. Values marked with daggers are found with randomized benchmarking[110]. Other values are rough experimental gate error estimates. In the case of photons, two-qubit gates fail frequently but success is heralded; error rates shown are conditional on a heralded success. NV, nitrogen vacancy.

Ladd, T. D., et al., Nature, 464(7285), 45–53, 2010

Progress in experimental QIP

- **# of qubits vs time**

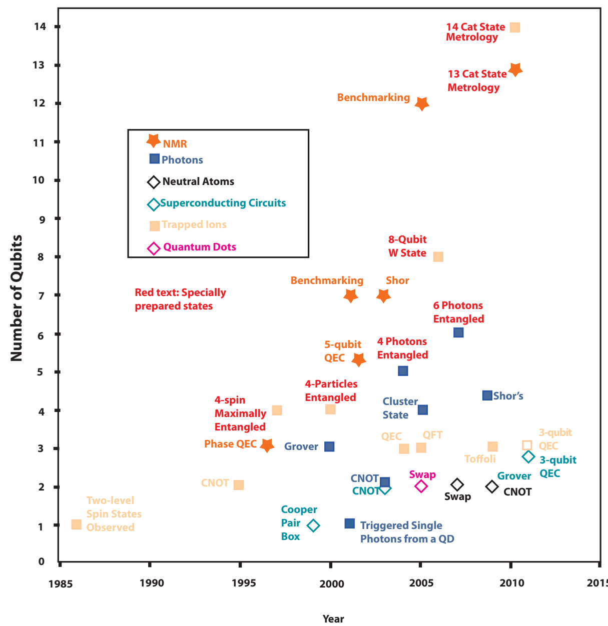

Adapted from Michael Mandelberg

yesterday we heard...

overhead: 10^3 is better than 10 ^11 ...

- **Increasing control of qubits**

Table 1 | Current performance of various qubits

Type of qubit	T_2	Benchmarking (%)		References
		One qubit	Two qubits	
Infrared photon	0.1 ms	0.016	1	20
Trapped ion	15 s	0.48†	0.7*	104–106
Trapped neutral atom	3 s	5		107
Liquid molecule nuclear spins	2 s	0.01†	0.47†	108
e^- spin in GaAs quantum dot	3 μs	5		43, 57
e^- spins bound to ^{31}P:^{28}Si	0.6 s	5		49
^{29}Si nuclear spins in ^{28}Si	25 s	5		50
NV centre in diamond	2 ms	2	5	60, 61, 65
Superconducting circuit	4 μs	0.7†	10*	73, 79, 81, 109

Measured T_2 times are shown, except for photons where T_2 is replaced by twice the hold-time (comparable to T_1) of a telecommunication-wavelength photon in fibre. Benchmarking values show approximate error rates for single or multi-qubit gates. Values marked with asterisks are found by quantum process or state tomography, and give the departure of the fidelity from 100%. Values marked with daggers are found with randomized benchmarking[110]. Other values are rough experimental gate error estimates. In the case of photons, two-qubit gates fail frequently but success is heralded; error rates shown are conditional on a heralded success. NV, nitrogen vacancy.

Ladd, T. D., et al., Nature, 464(7285), 45–53, 2010

Benchmarking gate

Usually we think of the circcuit model: Prepare a state, compute, measure

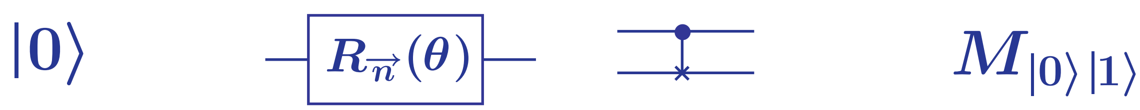

Other possibility is to use only generators of the Clifford group (generated by Hadamard, Phase gate and CNOT), with state preparation and measuremen in the computational basis:

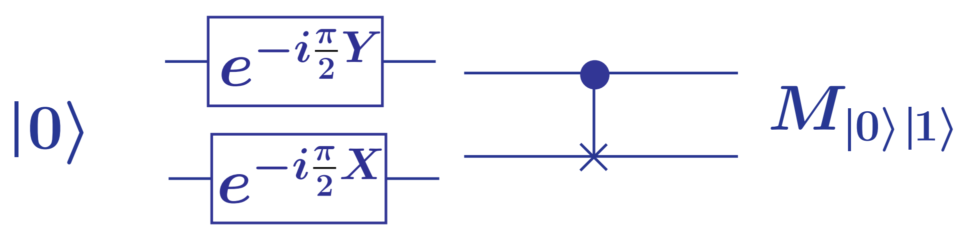

and include the preparation of

$$|\pi/8\rangle, or\ \rho = \frac{1}{2}\mathbb{1} + \frac{1}{\sqrt{3}}(X + Y + Z)$$

Benchmarking gates

Knill et. al. PRA, 77, 012307, (2008)

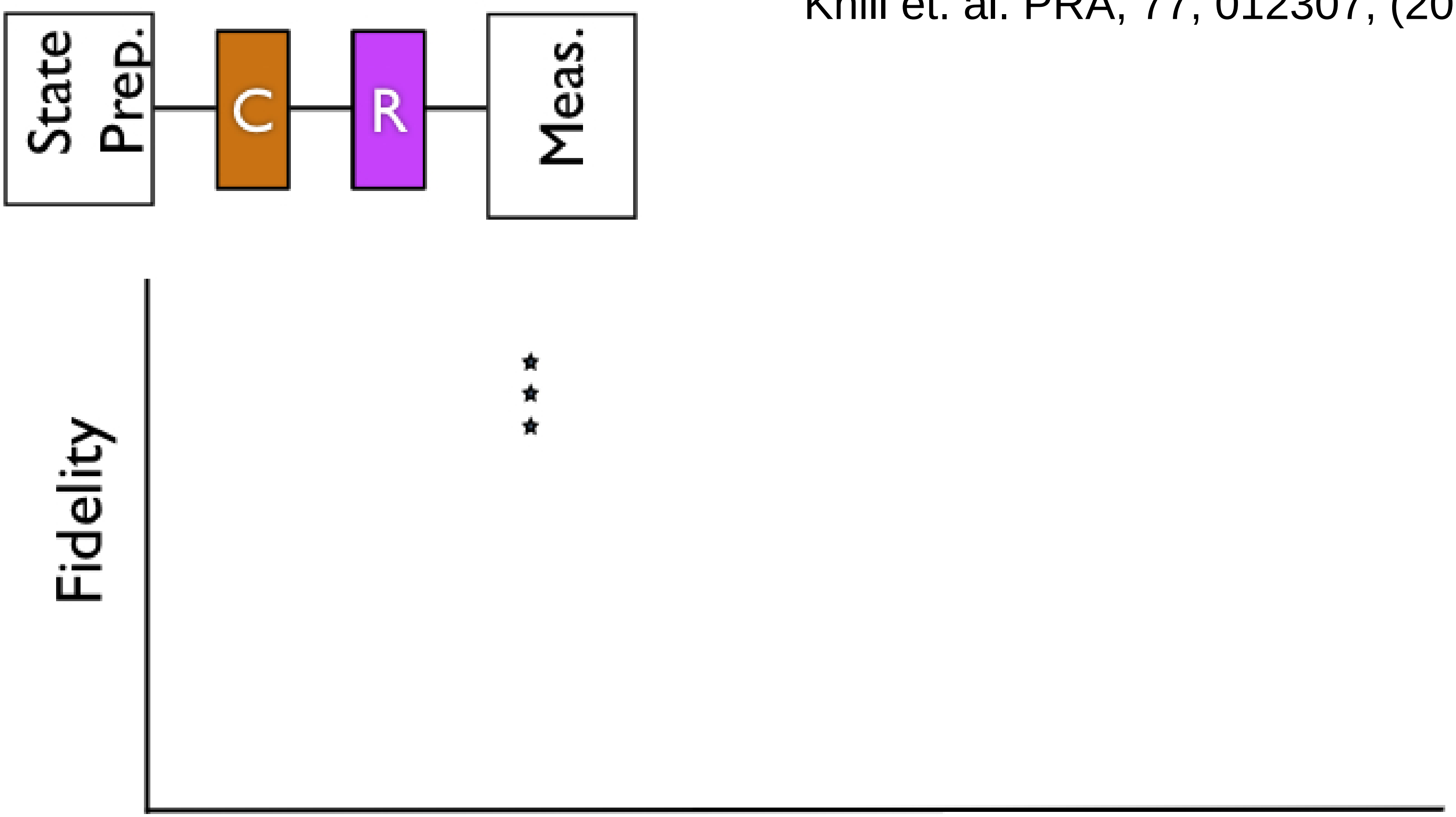

Benchmarking gates

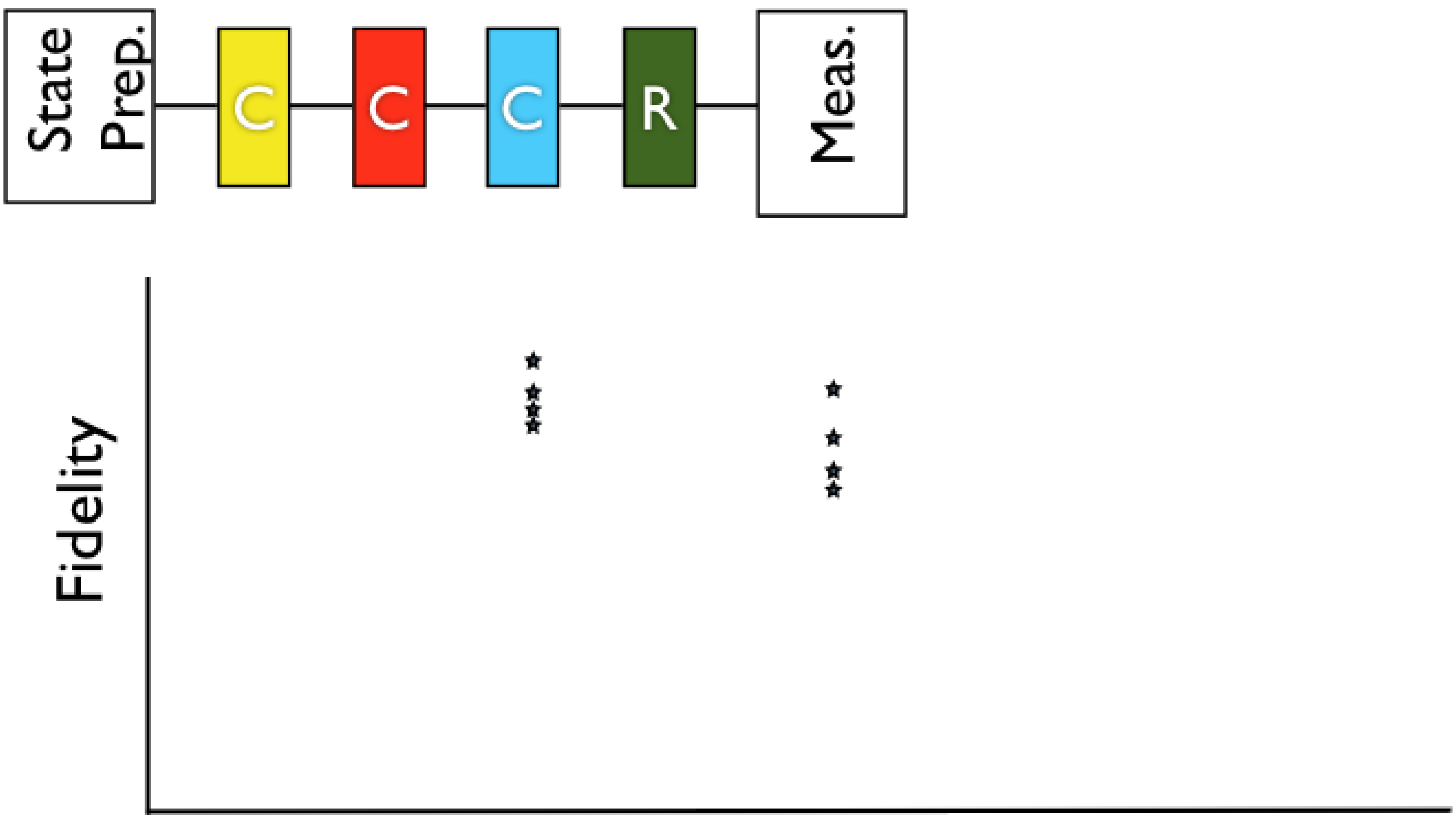

Benchmarking gates

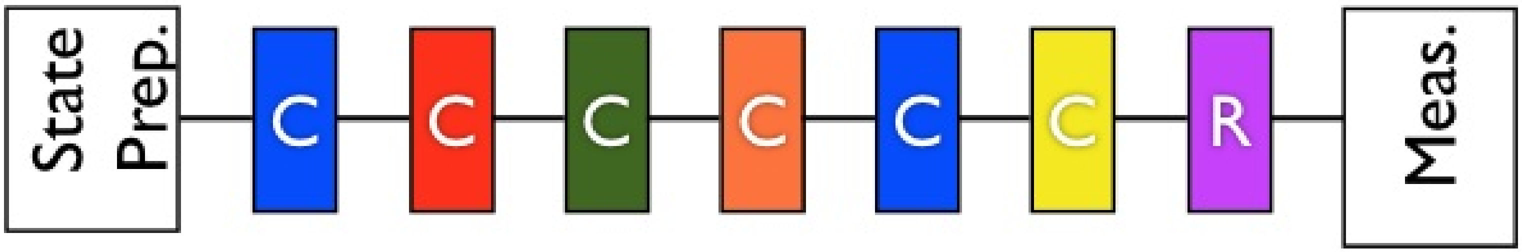

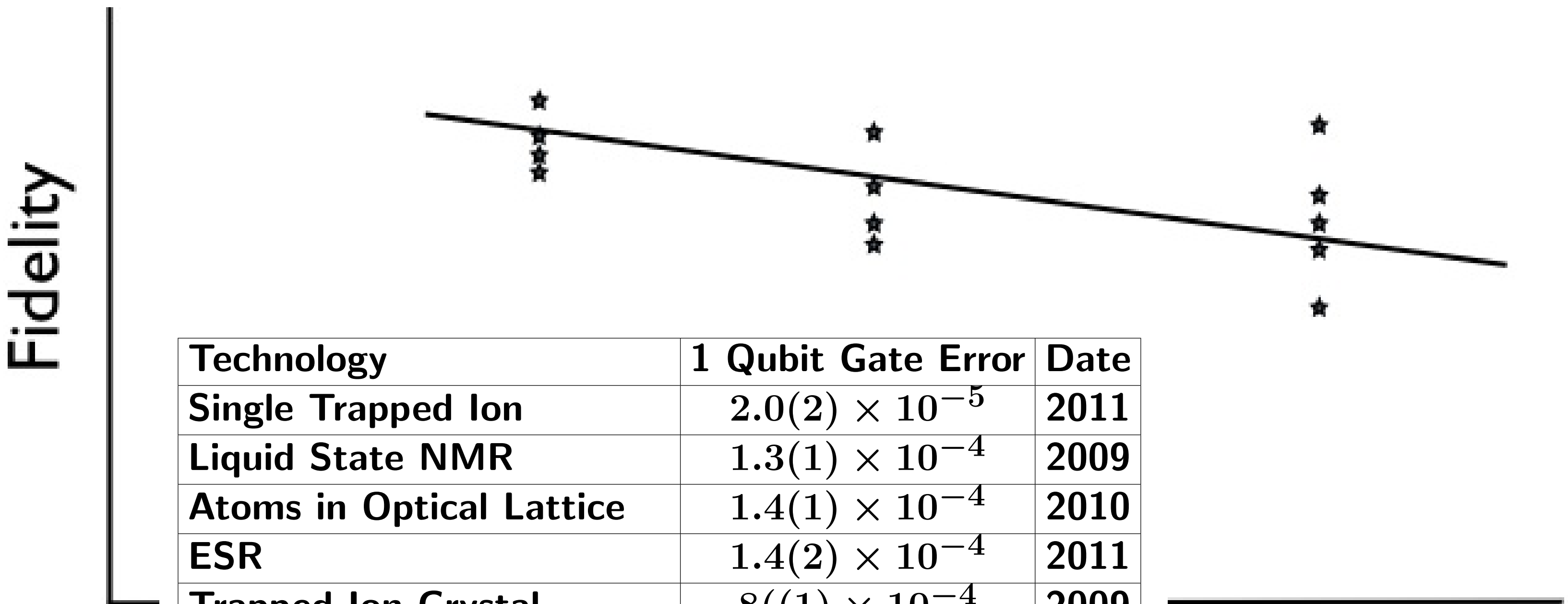

Technology	1 Qubit Gate Error	Date
Single Trapped Ion	$2.0(2) \times 10^{-5}$	2011
Liquid State NMR	$1.3(1) \times 10^{-4}$	2009
Atoms in Optical Lattice	$1.4(1) \times 10^{-4}$	2010
ESR	$1.4(2) \times 10^{-4}$	2011
Trapped Ion Crystal	$8((1) \times 10^{-4}$	2009
Single Trapped Ion	$4.8(2) \times 10^{-3}$	2008
Solid State NMR	$5(2) \times 10^{-3}$	2011
Superconducting Transmon	$7(5) \times 10^{-3}$	2010

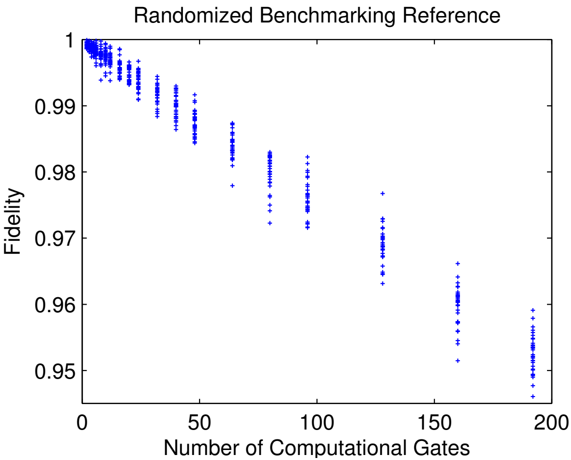
Randomized Benchmarking Reference
Fidelity
Number of Computational Gates
1
0.99
0.98
0.97
0.96
0.95
0
50
100
150
200

(a)

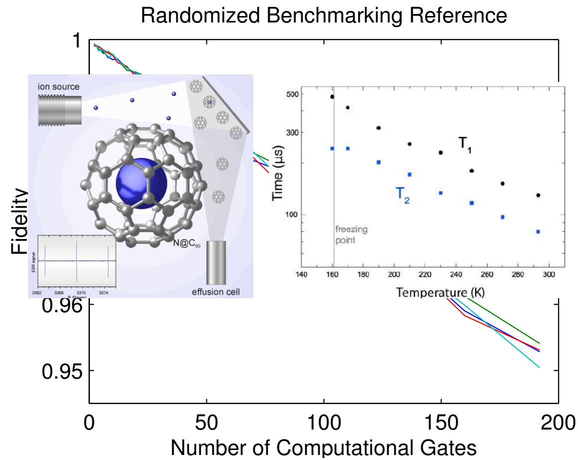
Randomized Benchmarking Reference
Fidelity
Number of Computational Gates
ion source
N@C60
effusion cell
Time (µs)
Temperature (K)
T1
T2
freezing point
500
300
100
140
160
180
200
220
240
260
280
300
1
0.96
0.95
0
50
100
150
200

(b)

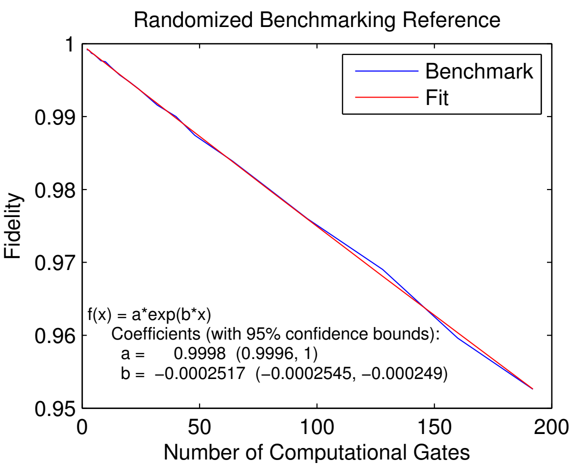
Randomized Benchmarking Reference
Benchmark
Fit
Fidelity
Number of Computational Gates
f(x) = a*exp(b*x)
Coefficients (with 95% confidence bounds):
a = 0.9998 (0.9996, 1)
b = −0.0002517 (−0.0002545, −0.000249)
1
0.99
0.98
0.97
0.96
0.95
0
50
100
150
200

(c)

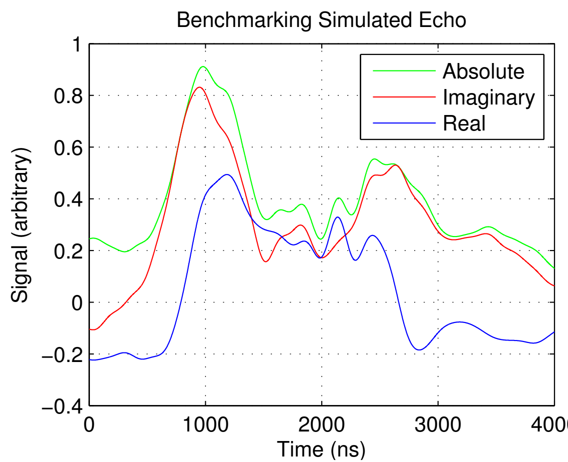
Benchmarking Simulated Echo
Absolute
Imaginary
Real
Signal (arbitrary)
Time (ns)
1
0.8
0.6
0.4
0.2
0
−0.2
−0.4
0
1000
2000
3000
4000

(d)

Benchmarking gates

Multi-qubit Comparison Summary Table

System	Error/Fidelty	Reference
liquid-state NMR	0.0047	NJP **11** 013034 (2009)
ion-trap (single)	99.3%	Nat. Phys. **4** 463 (2008)
superconducting	91%	Nature **460** 240 (2009)
NV centre	89%	Science **320** 1326 (2008)
Linear Optics	90%	PRL **93** 080502 (2004)
Neutral Atoms	73%	arXiv:0907.5552 (2009)
ESR	95%	Nature **455** 1085 (2008)

A generalisation of the 1 qubit benchmarking can be found in E. Magesan, J. M. Gambetta, and J. Emerson, Phys. Rev. Lett. 106, 180504 (2011).

Characterising noise in q. systems

Process tomography:

$$\rho_f = \sum_k A_k \rho_i A_k^\dagger = \sum_{kl} \chi_{kl} P_k \rho_i P_l$$

ıired as described by the

$$\begin{pmatrix} \rho^f_{\mathbb{1}} \\ \rho^f_X \\ \rho^f_Y \\ \rho^f_Z \end{pmatrix} = \begin{pmatrix} \chi_{\mathbb{1},\mathbb{1}} & \chi_{\mathbb{1},X} & \chi_{\mathbb{1},Y} & \chi_{\mathbb{1},Z} \\ \chi_{X,\mathbb{1}} & \chi_{X,X} & \chi_{X,Y} & \chi_{X,Z} \\ \chi_{Y,\mathbb{1}} & \chi_{Y,X} & \chi_{Y,Y} & \chi_{Y,Z} \\ \chi_{Z,\mathbb{1}} & \chi_{Z,X} & \chi_{Z,Y} & \chi_{Z,Z} \end{pmatrix} \begin{pmatrix} \rho^i_{\mathbb{1}} \\ \rho^i_X \\ \rho^i_Y \\ \rho^i_Z \end{pmatrix}$$

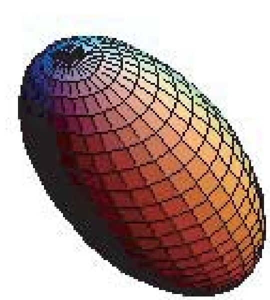

For n qubits, we need to provide $4^{2n} - 4^n$ numbers to do so.

Coarse graining

- We are not interested in all the elements that describe the full noise superopeartor but only a coarse graining of them.

- If we are interested in implementing quantum error corrrection, we can ask what is the probability to get one, or two, or k qubit error, independent of the location and independent of the type of error $\sigma_{x,y,z}$. The question is can we do this efficiently?

- Coarse graining is equivalent to implement a symmetry.

Emerson, Silva, Moussa, Ryan, Laforest, Baugh, Cory, Laflamme, Science 317, 1893, 2007

$$\Lambda(\rho) = \sum_{k}^{D^2} A_k \rho A_k^\dagger$$

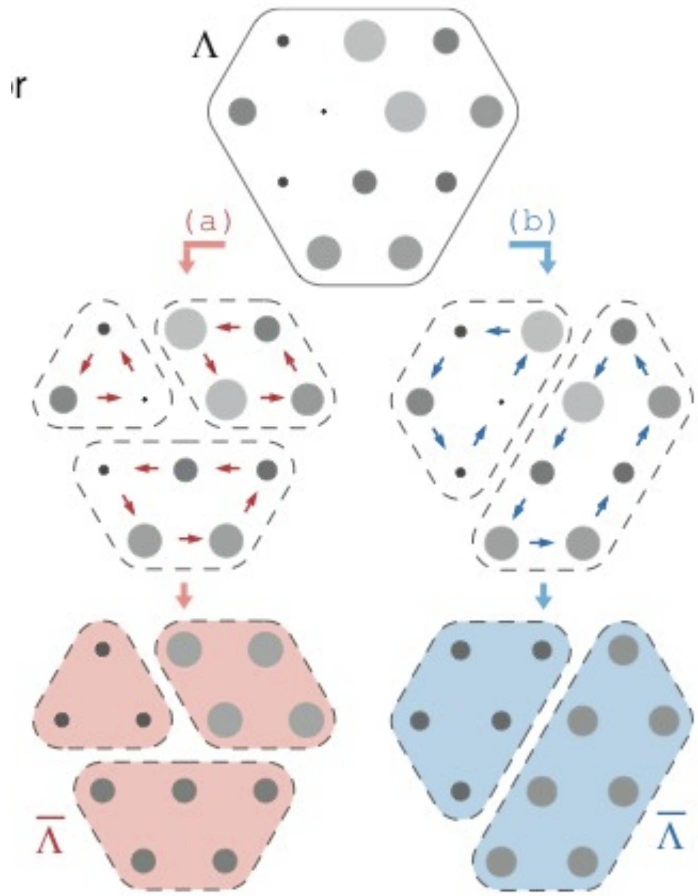

Schematic illustration of coarse-graining.

Coarse graining

1) we don't want to know which qubit is affected, coarse grain the position by symmetrising using permutation π_s

2) turn the noise into a depolarizing one for each qubit, coarse grain error type average over $SU(2)^{\otimes n}$

$$\rho_f = \sum_{kl} \chi_{kl} \int d\mu(U) U^\dagger P_k U \rho_i U^\dagger P_l^\dagger U$$

This is an example of a 2-design, and the integral can be replaced by a sum

$$\rho_f = \sum_{kl} \chi_{kl} \sum_{\alpha} C_\alpha^\dagger P_k C_\alpha \rho_i C_\alpha^\dagger P_l^\dagger C_\alpha$$

where C_α belongs to the Clifford group $\sim \mathcal{S}\mathcal{P}$ with $\mathcal{P} = \{\mathbb{1}, X, Y, Z\}$, $\mathcal{S} = \{e^{-i\frac{\pi}{4}X}, e^{-i\frac{\pi}{4}Y}, e^{-i\frac{\pi}{4}Z}\}$

Coarse graining

To estimate the noise, start with the state $|000\ldots\rangle$, implement the symmetrisation group and the Clifford group and count how many bits have been flipped.

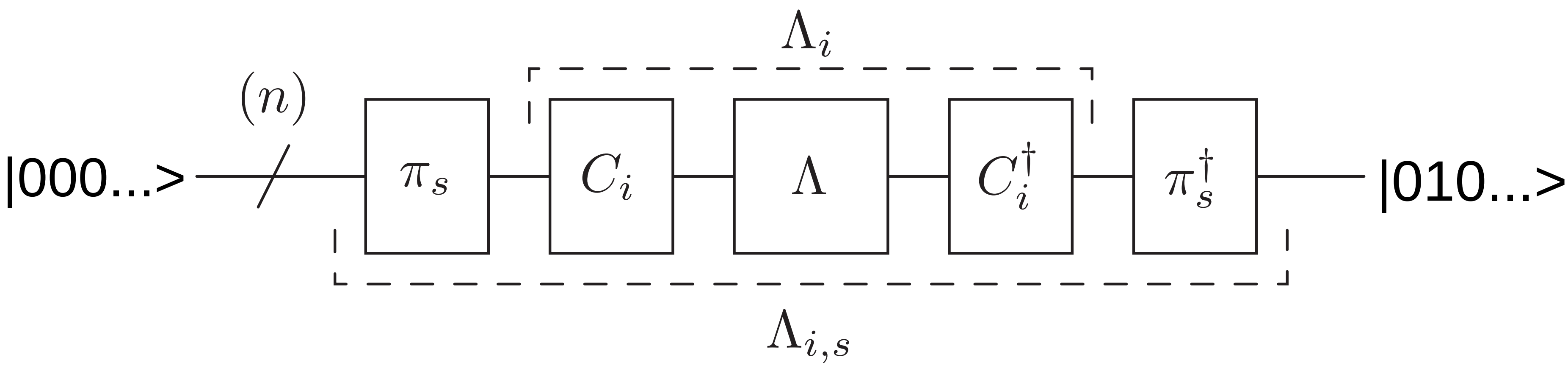

If we implement all the elements in the Clifford and permutation group, we would have an exponential number of terms , but the sum can be estimated by sampling and using the Chernoff bound. **(see Emerson et al. Science 317, 1893, 2007)**

Errors in Clifford gates

Adapt the idea for Clifford gates

Practical experimental certification of computational quantum gates via twirling O. Moussa, M.P. da Silva, C.A. Ryan and R. Laflamme

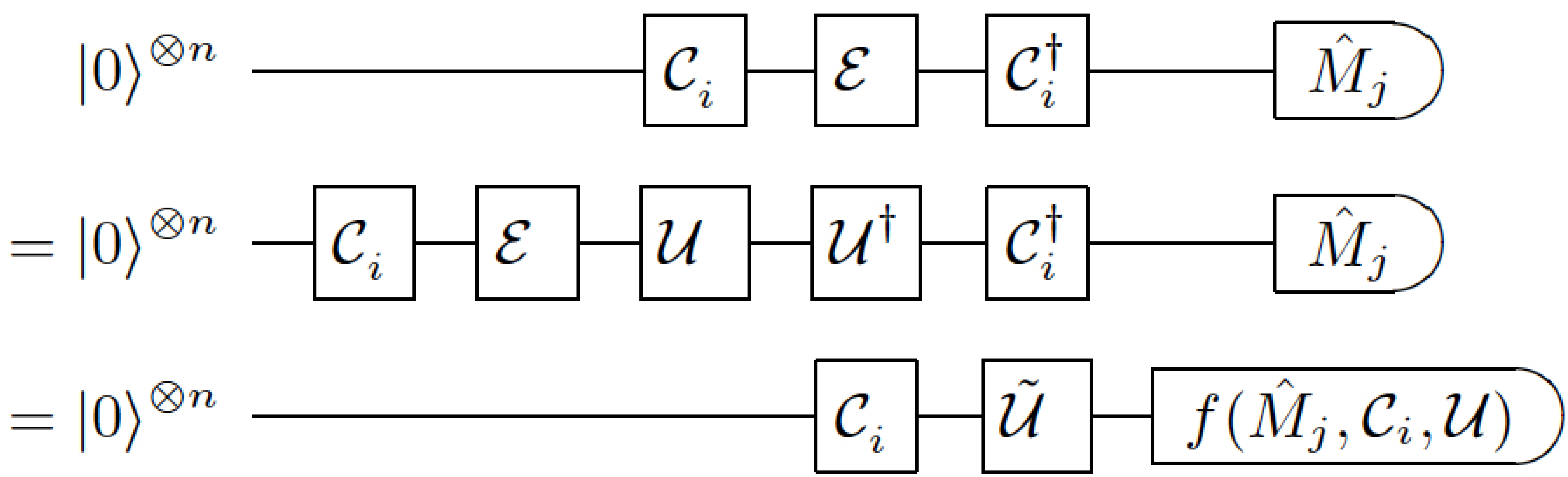

Errors in Clifford gates

Use malonic acid in solid state

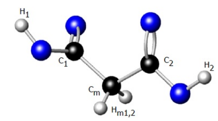

kHz	C_1	C_2	C_m
C_1	6.380	0.297	0.780
C_2	-0.025	-1.533	1.050
C_m	0.071	0.042	-5.650

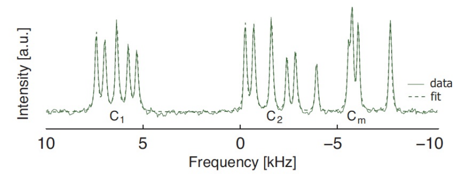

One qubit can be benchmarked using the Knill procedure:

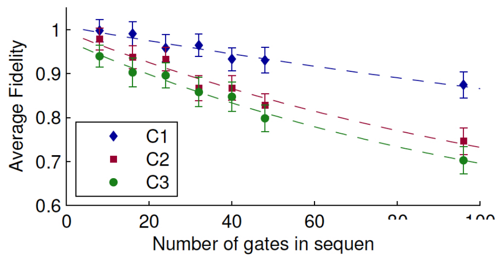

and Clifford gates using the new procedure

	Target	Experiment	w	k_w	λ_w	$\bar{F}$
a		prep	1	6	0.967 ± 0.010	$0.983^{+0.007}_{-0.006}$
			2	21	1.000 ± 0.009	
			3	7	0.978 ± 0.017	
b		prep, unrectified pulse	1	8	0.848 ± 0.022	$0.863^{+0.013}_{-0.012}$
			2	21	0.883 ± 0.017	
			3	8	0.799 ± 0.023	
c		prep, rectified pulse	1	6	0.959 ± 0.014	$0.973^{+0.009}_{-0.008}$
			2	21	0.989 ± 0.013	
			3	8	0.964 ± 0.016	

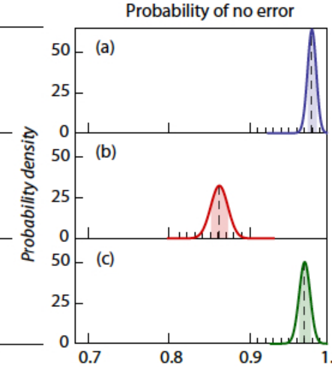

Note: the difference between b) and c) is improving the pulse ("fixing")

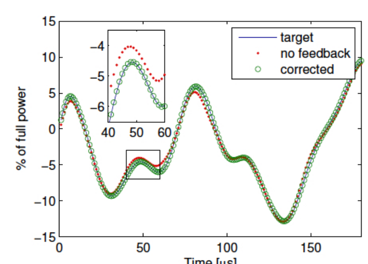

VOLUME 81, NUMBER 10 PHYSICAL REVIEW LETTERS 7 SEPTEMBER 1998

Experimental Quantum Error Correction

D. G. Cory,[1] M. D. Price,[2] W. Maas,[3] E. Knill,[4] R. Laflamme,[4] W. H. Zurek,[4] T. F. Havel,[5] and S. S. Somaroo[5]

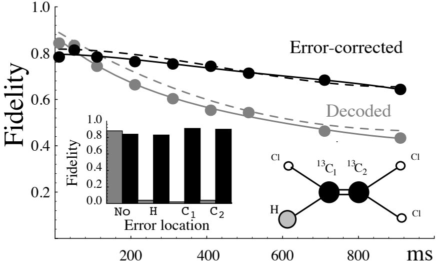

FIG. 3. Experimentally determined entanglement fidelities for the TCE experiments after decoding (gray) and after decoding and error correction (black). The relevant coupling frequencies

T_2: H= 3s , C_1=1.1s, C_2=0.6s

DE: $0.85 - 1.10\ t + O(t^2)$

EC: $0.79 - 0.09\ t + O(t^2)$

$\Longrightarrow\ >$ order of magnitude improvement in 1^{st} order.

PHYSICAL REVIEW A **84**, 034303 (2011)

Experimental quantum error correction with high fidelity

Jingfu Zhang,[1] Dorian Gangloff,[1,*] Osama Moussa,[1] and Raymond Laflamme[1,2]

		H	C_1	C_2
(a)	H	-4546.6		
	C_1	201.4	-20529.5	
	C_2	8.5	103.1	-21789.5
(b)	T_1(s)	8.9±0.3	8.9±0.3	13.0±0.3
	T_2(s)	1.7±0.2	1.18±0.02	0.45±0.02

FIG. 1. Parameters of the spin qubits. (a) Chemical shifts shown as the diagonal terms and the couplings between spins shown as the nondiagonal terms in Hz. The inset shows the molecule structure where the three qubits are H, C_1, and C_2. (b) The relaxation times T_1 are measured by the standard inversion recovery sequence. T_2's are measured by the Hahn echo with one refocusing pulse, by ignoring the strong coupling in the Hamiltonian (1).

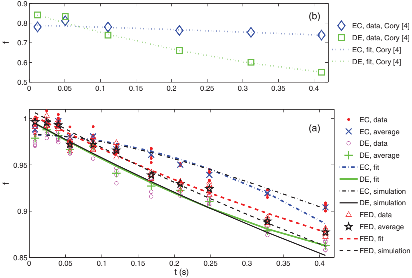

FIG. 3. (Color online) (a) Experimental results for error correction (EC), decoding (DE), and free evolution decay (FED). For each delay time, we take five data points by repeating experiments, shown as • for EC, ○ for DE, and △ for FED. The averages are shown as ×, +, and ⋆, which can be fitted as $0.9828 - 0.0166t - 0.5380t^2 + 0.0014t^3$ with relative fitting error 0.73%, $0.9982 - 0.4361t + 0.1679t^2 + 0.2152t^3$ with relative fitting error 0.57%, and $1.0056 - 0.4164t + 0.3363t^2 - 0.2123t^3$ with relative fitting error 0.45%, shown as the thick dash-dotted, solid, and dashed curves, respectively. The ratios of the first-order decay terms in the fitted curves are calculated as 26.2 ± 0.3 for DE and EC, and 25.0 ± 0.3 for FED and EC, respectively. The thin dash-dotted, solid, and dashed curves show the fitting results using the ideal data points from simulation by introducing factors of 0.983 ± 0.006, 0.998 ± 0.007, and 1.0098 ± 0.0064 for EC, DE, and FED, respectively. (b) Results in the previous experiment [4], shown as the data marked by ⋄ and □ for EC and DE, which can be fitted as $0.7895 - 0.0957t - 0.0828t^2 + 0.0370t^3$ and $0.8539 - 1.1021t + 0.8696t^2 + 0.0378t^3$ with relative fitting errors 0.89% and 0.98%, respectively. The ratio of the first-order decay terms is 11.5 ± 0.2.

Summary

1998:
T_2: H= 3s , C_1=1.1s, C_2=0.6s
DE: $0.85 - 1.10\ t + O(t^2)$
EC: $0.79 - 0.09\ t + O(t^2)$

2011:
T_2: H= 1.7s , C_1=1.18s, C_2=0.45s
DE: $0.99 - 0.436\ t + O(t^2)$
EC: $0.98 - 0.017\ t + O(t^2)$

Comparison:

- Zeroth order improved by $\sim$ **20%**
- First order is reduced further, from **11** fold (91% removed) to **26** fold ($>$ 96% removed)

$$F = \sum_{\mu} p_{\mu} |\mathrm{Tr}[U^{\dagger}_{\mathrm{des}} U^{\mu}_{\mathrm{cal}}]/N|^2$$

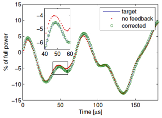

with

$$U^{\mu}_{cal} = U(t) = e^{-i \int_0^t (H^{\mu}_{B_o} + H_{int} + H^{\mu}_{rf}(t)) dt}$$

Superconducting qubits: 3 qubit coo

Realization of Three-Qubit Quantum Error Correction with Superconducting Circuits; M. D. Reed et al. arXiv:1109.4948

- **Performed both the bit flip and phase flip error correction (in separate experiments)**

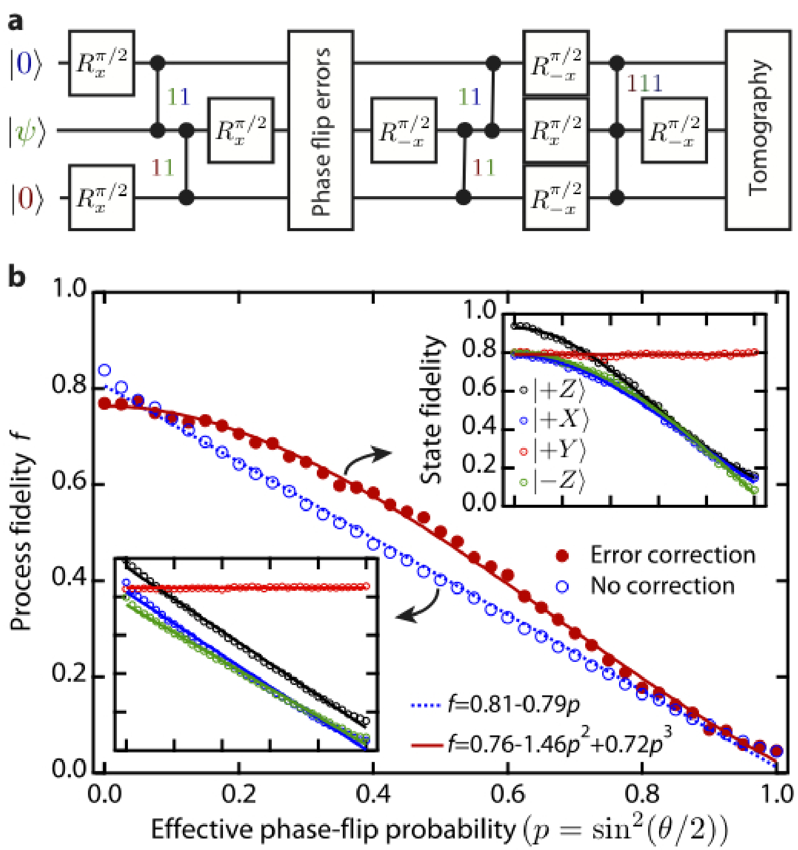

- **Errors on all three qubits simultaneously with z-gates of known rotation angle, which is equivalent to phase-flip errors with probability $p = \sin^2(\theta/2)$.**
- **The process fidelity is fit with $f = 0.81 - 0.79p$ without QEC and $f = (0.76 \pm 0.005)(1.46 \pm 0.03)p^2 + (0.72 \pm 0.03)p^3$ with QEC. If a linear term is allowed, its best-fit coefficient is $(0.03 \pm 0.06)p$.**

PRL **107,** 160501 (2011) PHYSICAL REVIEW LETTERS week ending 14 OCTOBER 2011

Demonstration of Sufficient Control for Two Rounds of Quantum Error Correction in a Solid State Ensemble Quantum Information Processor

Osama Moussa,[1,2,*] Jonathan Baugh,[1,3] Colm A. Ryan,[1,2] and Raymond Laflamme[1,2,4]

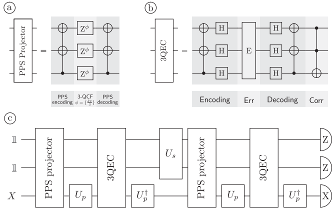

FIG. 1. Shown are the implemented quantum circuits for: (a) labeled PPS preparation procedure: a 3QCF is conjugated by a unitary operation that encodes (and decodes) the labeled pseudopure state $|00\rangle\langle 00|X$ in the triple quantum coherence $|000\rangle\langle 111| + |111\rangle\langle 000|$; (b) the implemented quantum circuit of a 3-qubit QECC, showing the encoding, decoding, and error-correction steps. The top two qubits are initialized to the $|00\rangle$ state, and the bottom qubit carries the information to be encoded. After the decoding and correction operations, the bottom qubit is restored to its initial state, while the top two qubits carry information about which error had occurred; and (c) the procedure for two rounds: U_p prepares X, Y, or Z inputs, and $U_s = \{II, XI, IX, XX\}$ toggles between the different syndrome subspaces; i.e., the experiment is repeated 4 times, cycling through the different U_s, and then the results are added, similar to a standard phase cycling procedure.

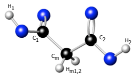

kHz	C_1	C_2	C_m
C_1	6.380	0.297	0.780
C_2	-0.025	-1.533	1.050
C_m	0.071	0.042	-5.650

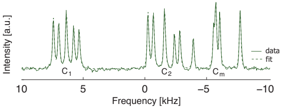

FIG. 2. Malonic acid ($C_3H_4O_4$) molecule and Hamiltonian parameters (all values in kHz). Elements along the diagonal represent chemical shifts, ω_i, with respect to the transmitter frequency (with the Hamiltonian $\sum_i \pi\omega_i Z_i$). Above the diagonal are dipolar coupling constants ($\sum_{i<j} \pi D_{i,j}(2\ Z_iZ_j - X_iX_j - Y_iY_j)$, and below the diagonal are J coupling constants, ($\sum_{i<j} \frac{\pi}{2} J_{i,j}(Z_iZ_j + X_iX_j + Y_iY_j)$. An accurate natural Hamiltonian is necessary for high fidelity control and is obtained from precise spectral fitting of (also shown) a proton-decoupled ^{13}C spectrum following polarization-transfer from the abundant protons. The central peak in each quintuplet is due to natural abundance ^{13}C nuclei present in the crystal at $\sim 1\%$. (for more details see [7, 10] and references therein.)

PRL **107,** 160501 (2011) PHYSICAL REVIEW LETTERS week ending 14 OCTOBER 2011

Demonstration of Sufficient Control for Two Rounds of Quantum Error Correction in a Solid State Ensemble Quantum Information Processor

Osama Moussa,[1,2,*] Jonathan Baugh,[1,3] Colm A. Ryan,[1,2] and Raymond Laflamme[1,2,4]

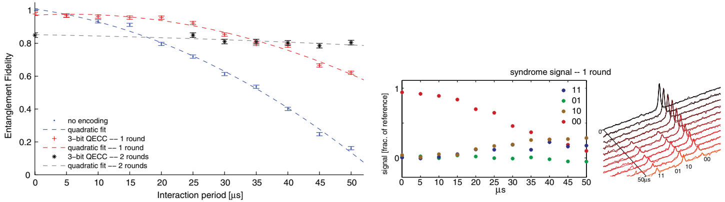

FIG. 4 (color online). Summary of experimental results for the *partial decoupling* map: the system evolves under the natural Hamiltonian as well as 70 kHz decoupling fields that partially modulate the heteronuclear interactions (between the carbons and protons). Shown (on left) are the single-qubit entanglement fidelities in the cases where no encoding is employed (blue dots); or one round of the 3-bit code (red crosses); or two rounds of the 3-bit code (black asterisks), where the interaction interval is split to two equal intervals. The dashed lines are quadratic fits to the data and are included to guide the eye. Also shown (on right) is the signal after one round of error correction as distributed over the various error-syndrome subspaces. In this case, the dominant errors are phase flips on the top and bottom qubits, which are encoded on C_1 and C_m, respectively.

SCIENCE VOL 332 27 MAY 2011 1059

Experimental Repetitive Quantum Error Correction

Philipp Schindler,[1] Julio T. Barreiro,[1] Thomas Monz,[1] Volckmar Nebendahl,[2] Daniel Nigg,[1] Michael Chwalla,[1,3] Markus Hennrich,[1*] Rainer Blatt[1,3]

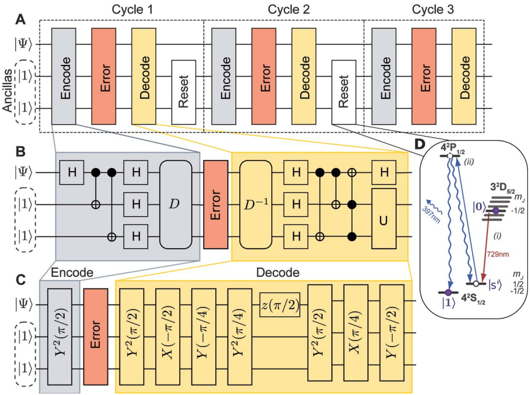

Fig. 1. (**A**) Schematic view of three subsequent error-correction cycles. (**B**) Quantum circuit for the implemented phase-flip error-correction code. The operations labeled H are Hadamard gates. (**C**) Optimized pulse sequence implementing a single error-correction cycle. (**D**) Schematic of the reset procedure. The computational qubit is marked by filled dots. The reset procedure consists of (i) shelving the population from $|0\rangle$ to $|s'\rangle = 4S_{1/2}(m_J = +1/2)$ and (ii) optical pumping to $|1\rangle$ (straight blue arrow).

SCIENCE VOL 332 27 MAY 2011 1059

Experimental Repetitive Quantum Error Correction

Philipp Schindler,[1] Julio T. Barreiro,[1] Thomas Monz,[1] Volckmar Nebendahl,[2] Daniel Nigg,[1] Michael Chwalla,[1,3] Markus Hennrich,[1*] Rainer Blatt[1,3]

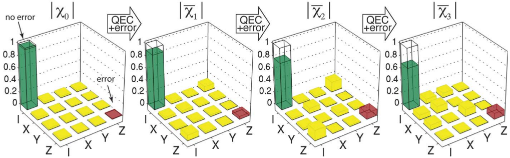

Fig. 2. Mean single-qubit process matrices $\overline{\chi}_n$ (absolute value) for n QEC cycles with single-qubit errors. Transparent bars show the identity process matrix, and the red bar denotes a phase-flip error. These process matrices were reconstructed from a data set averaged over all possible single-qubit errors.

Table 1. Process fidelity for a single uncorrected qubit as well as for one, two, and three error-correction cycles. F_{none} is the process fidelity without inducing any errors. F_{single} is obtained by averaging over all single-qubit errors. F_{opt} and F_{sopt} are the respective process fidelities where constant operations are neglected. The statistical errors are derived from propagated statistics in the measured expectation values where the numbers in parentheses indicate one standard deviation. Dash entries indicate not applicable.

Number of QEC cycles	No error F_{none}	Optimized no error F_{opt}	Single-qubit errors F_{single}	Optimized single-qubit errors F_{sopt}
0	97(2)	97(2)	–	–
1	87.5(2)	90.1(2)	89.1(2)	90.1(2)
2	77.7(4)	79.8(4)	76.3(2)	80.1(2)
3	68.3(5)	72.9(5)	68.3(3)	70.2(3)

SCIENCE VOL 332 27 MAY 2011 1059

Experimental Repetitive Quantum Error Correction

Philipp Schindler,[1] Julio T. Barreiro,[1] Thomas Monz,[1] Volckmar Nebendahl,[2] Daniel Nigg,[1]
Michael Chwalla,[1,3] Markus Hennrich,[1*] Rainer Blatt[1,3]

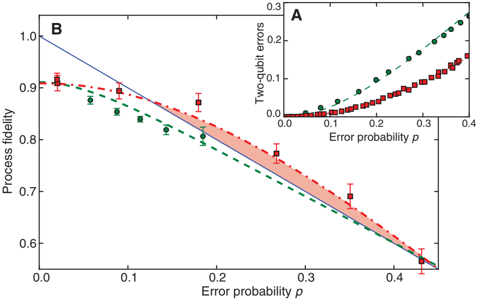

Fig. 3. (**A**) Probability of simultaneous two-qubit phase flips as a function of the single-qubit phase flip probabilities for uncorrelated (square) and correlated (circle) noise measured by a Ramsey-type experiment. (**B**) Process fidelity of the QEC algorithm in the presence of correlated (circle) and uncorrelated (square) phase noise as a function of the single-qubit phase flip probability. The theory is shown for an unencoded qubit (solid line), a corrected qubit in presence of correlated (dashed line), and uncorrelated noise (dash-dot line). Error bars indicate one standard deviation derived from propagated statistics in the measured expectation values.

Erasure-correcting code in optics

C-Y Lu et al. Proc. Natl. Acad. Sci. USA 105, 11050-11054 (2008)

Encoding:

$$|0\rangle_L = (|00\rangle_{12} + |11\rangle_{12})(|00\rangle_{34} + |11\rangle_{34})$$
$$|1\rangle_L = (|00\rangle_{12} - |11\rangle_{12})(|00\rangle_{34} - |11\rangle_{34})$$

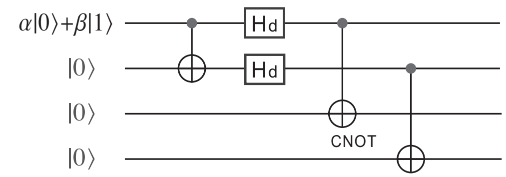

FIG. 1: A quantum circuit with two Hadamard (H_d) gates and three CNOT gates for implementation of the four-qubit QEEC code. The stabilizer generators of the QEEC code are $X \otimes X \otimes X \otimes X$ and $Z \otimes Z \otimes Z \otimes Z$, where X (Z) is short for Pauli matrix σ_x (σ_z) [24]. As proposed by Vaidman *et al.*, this four-qubit code can also be used for error detection [33].

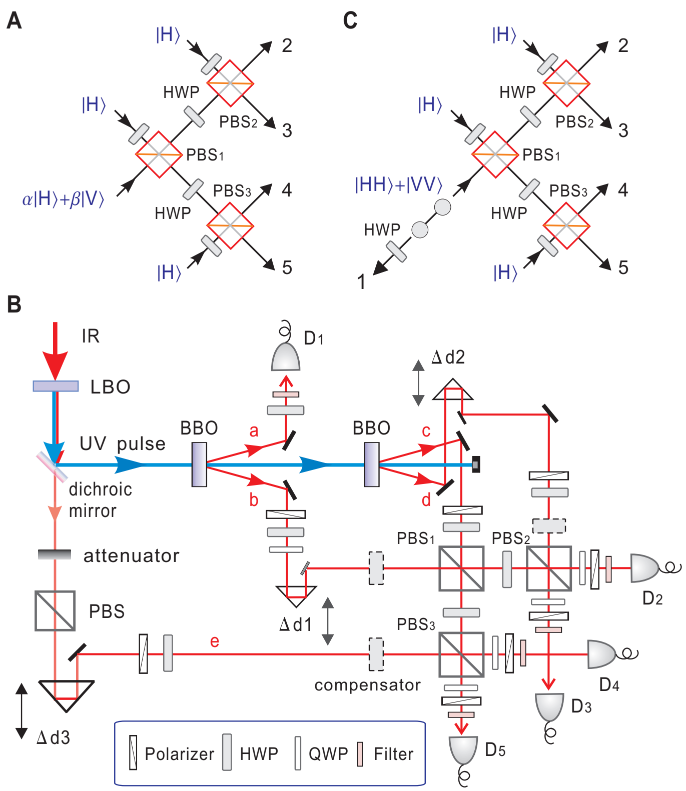

Test the code with the encoded states

$$|V\rangle_L = (|HH\rangle_{23} - |VV\rangle_{23})(|HH\rangle_{45} - |VV\rangle_{45})$$

$$|+\rangle_L = (|HHHH\rangle_{2345} + |VVVV\rangle_{2345}$$

$$|R\rangle_L = (|HH\rangle_{23} + |VV\rangle_{23})(|HH\rangle_{45} + |VV\rangle_{45}) + (|HH\rangle_{23} - |VV\rangle_{23})(|HH\rangle_{45} - |VV\rangle_{45})$$

For input states $|V\rangle_L$, $|+\rangle_L$ and $|R\rangle_L$, the recovery fidelities averaged over all possible measurement outcomes are found to be 0.832 ± 0.012, 0.764 ± 0.014, and 0.745 ± 0.015 demonstrating error correction.

Erasure-correcting code in optics

M. Lassen et al. Nature Photonics 4, 700, 2010

Error model: random fading, likely to occur as a result of time jitter noise or beam pointing noise in an atmospheric transmission channel and can be represented by $\rho = (1 - P_E)|\alpha\rangle\langle\alpha| + P_E|0\rangle\langle 0|$

NATURE PHOTONICS DOI: 10.1038/NPHOTON.2010.168 LETTERS

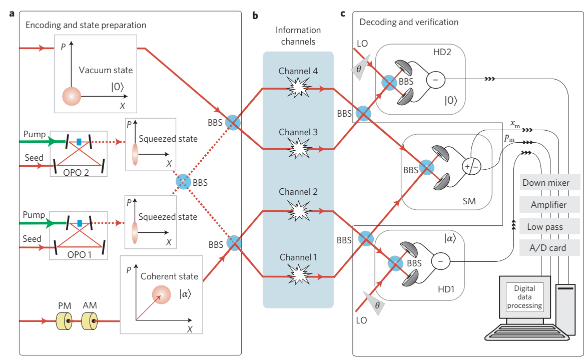

Figure 1 | Schematics of the experimental QECC set-up. a, The four-mode code is prepared through linear interference at three balanced beamsplitters (BBS) between the two input states, $|\alpha\rangle$ and $|0\rangle$, and two ancillary squeezed vacuum states. The latter states are produced in two optical parametric oscillators, OPO 1 and OPO 2, and the coherent state is prepared via a coherent modulation at 5.5 MHz produced by an amplitude (AM) and a phase modulator (PM). **b**, The encoded state is injected into four free-space channels that can be independently blocked, thereby mimicking erasures. **c**, The corrupted state is decoded, the error is detected by the syndrome measurement (SM) and the state is deterministically corrected or probabilistically selected. The measurement is an entangled measurement in which the phase and amplitude quadratures of the two emerging states are jointly measured (for example, see ref. 25). The error correcting displacement or post-selection operation is carried out electronically after the measurement of the transmitted quantum states. These states are measured with two independent homodyne detectors that allow for full quantum state characterization, by scanning the phases (θ) of the local oscillators (LOs) with respect to the phases of the signals. All erasure events are obtained by blocking the beam paths.

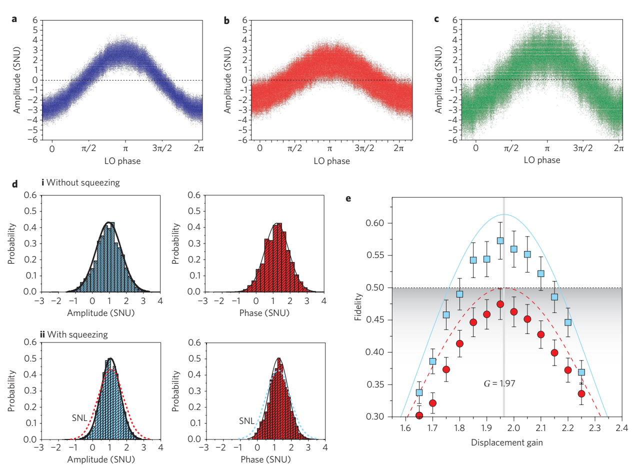

Figure 2 | Results of the deterministic QECC protocol. a, Phase scan of the input coherent state with the excitation $|\alpha\rangle \approx |3+3i\rangle$. **b**,**c**, Phase scans of the output state measured at HD1 before correction (**b**) and of the corrected output state (**c**). **d**, Histograms of the marginal distributions of the amplitude and phase quadratures of the joint syndrome measurement (in shot noise units, SNU). Red and blue curves correspond to the marginal distributions for a shot-noise-limited (SNL) state, whereas the black curves are the best Gaussian fits to the histograms. **e**, Fidelity is plotted as a function of the displacement gain with (blue squares) and without (red circles) the use of entanglement. The dashed and solid lines are the theoretically predicted fidelities for 0 dB and 2 dB of two-mode squeezing, respectively. The error bars depend on the measurement error, which is mainly associated with the stability of the system over time and the finite resolution of the analog-to-digital converter. This amounts to an error of $\pm 3\%$ for all fidelities.

The CV code for protecting quantum information from erasures is a four-mode entangled mesoscopic state in which two (information-carrying) quantum states are encoded with the help of a two-mode entangled vacuum state

DFS in neutron interferometry

D. Pushin, et al. PRL 107.150401, 2011

Neutron are great probes to
- **characterize magnetic, nuclear and structural properties of materials, protein structures**
- **can be used on biological or cold material,**
- **but they lack robustness**

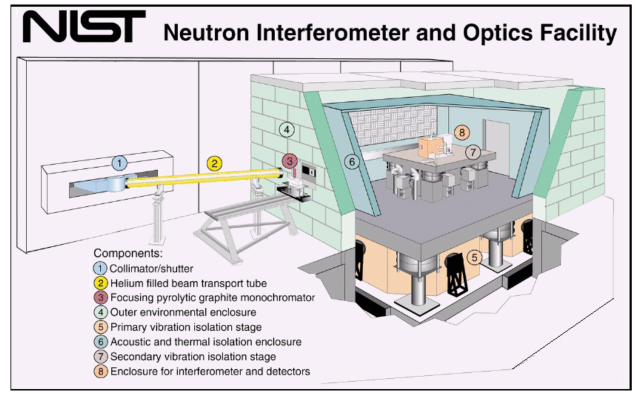

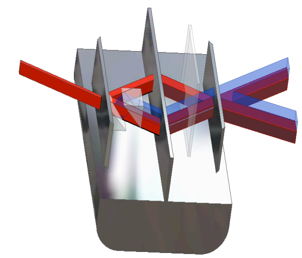

From an information processing point of view:

$$|01\rangle \rightarrow \frac{1}{\sqrt{2}}(|01\rangle + |10\rangle) \rightarrow \alpha|01\rangle + \beta|10\rangle$$

or in "logical" terms:

$$|0_L\rangle \rightarrow \frac{1}{\sqrt{2}}(|0_L\rangle + |1_L\rangle) \rightarrow \alpha|0_L\rangle + \beta|1_L\rangle$$

The dominant noise is a phase shift due to rotation around the vertical axis, i.e. $e^{i\theta Z}$

DFS in neutron interferometry

D. Pushin, et al. PRL 107.150401, 2011

In the 4(or 5)-blade case we have path 1 and path 2 canceling each other phase gain/loss and this is similar to 2 qubit system subject to the noise $Z_1 Z_2$ which has a DFS $\{|01_L\rangle, |10_L\rangle\}$.

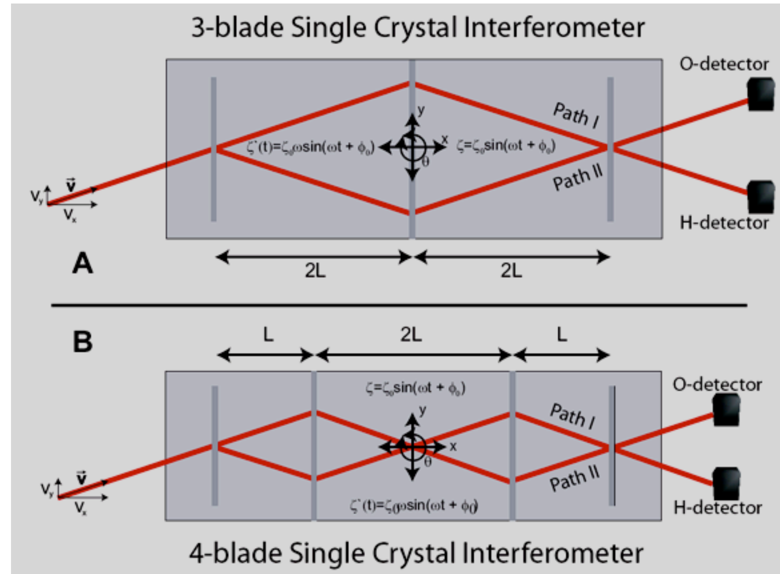

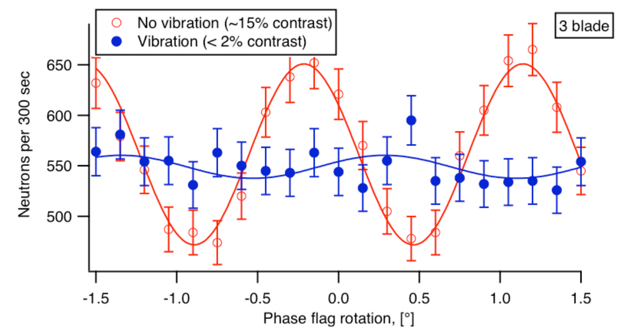

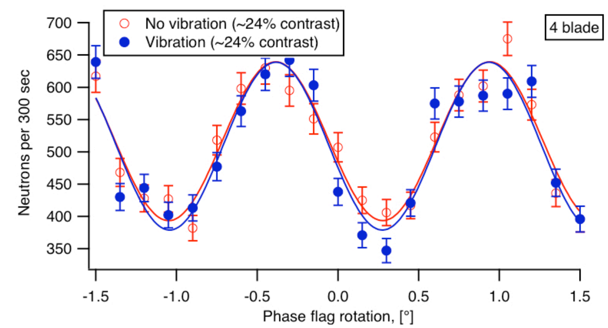

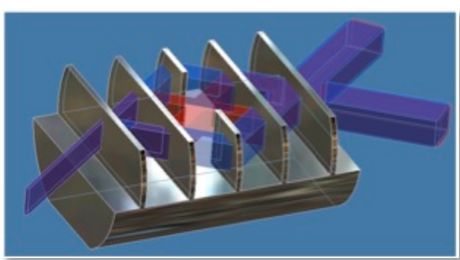

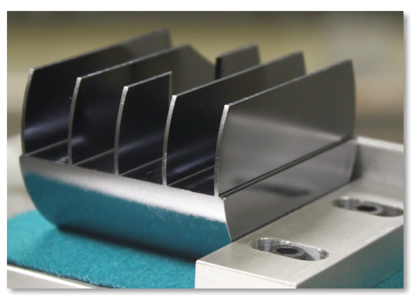

Magic state distillation

Kitaev and Bravyi Phys. Rev. A 71 (2005) 022316

If ρ has imperfection such as

$$\rho' = \frac{1}{2}\mathbb{1} + \frac{p'}{\sqrt{3}}(X + Y + Z)$$

we can use the decoding of 5 bit code to purify the state

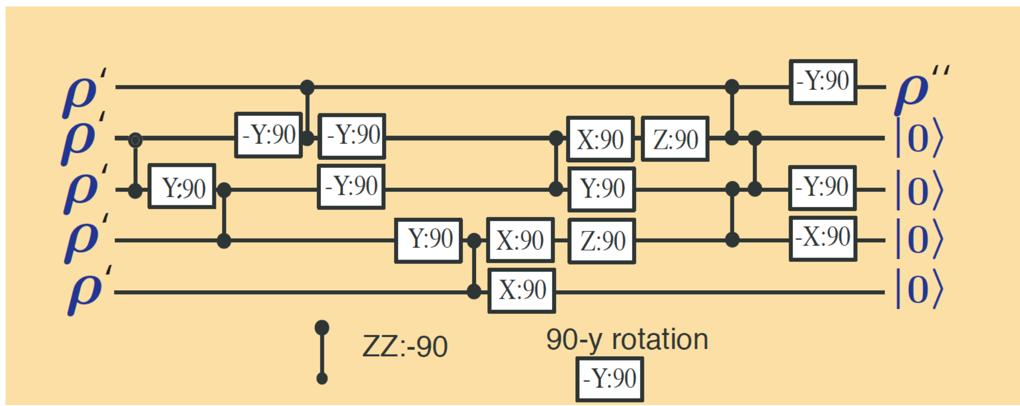

i.e., if p' is near enough 1, $p'' > p'$

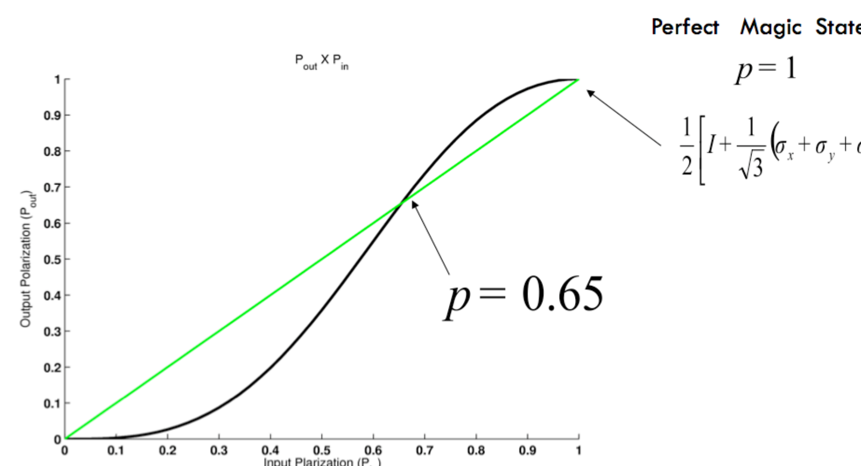

Magic state distillation

Kitaev and Bravyi Phys. Rev. A 71 (2005) 022316

If ρ has imperfection such as

$$\rho' = \frac{1}{2}\mathbb{1} + \frac{p'}{\sqrt{3}}(X + Y + Z)$$

we can use the decoding of 5 bit code to purify the state

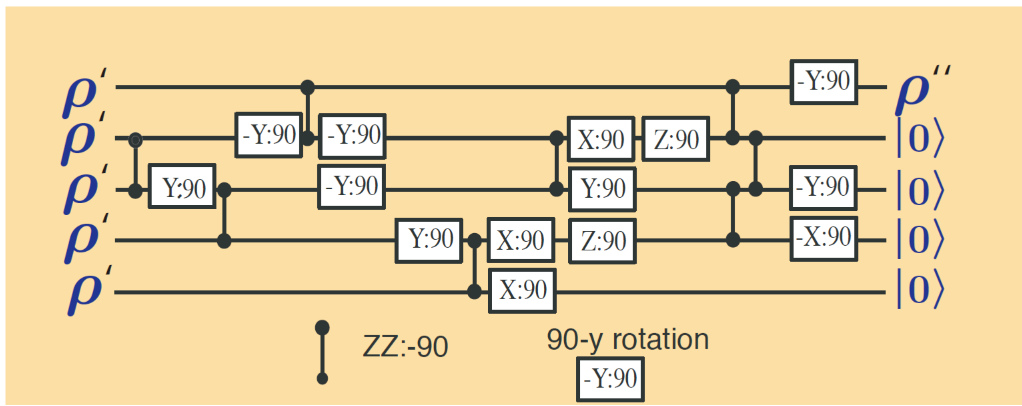

i.e., if p' is near enough 1, $p'' > p'$

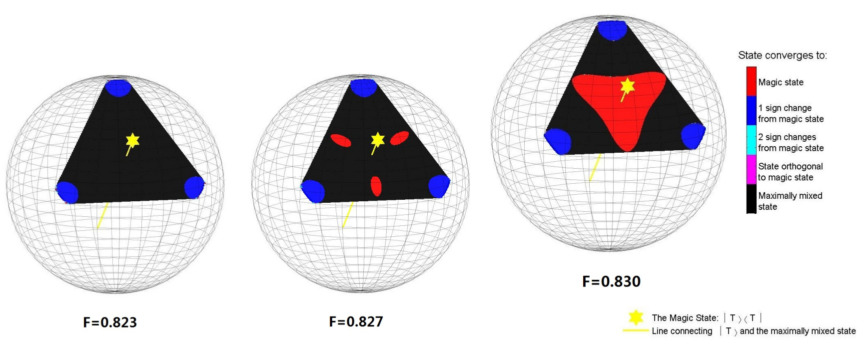

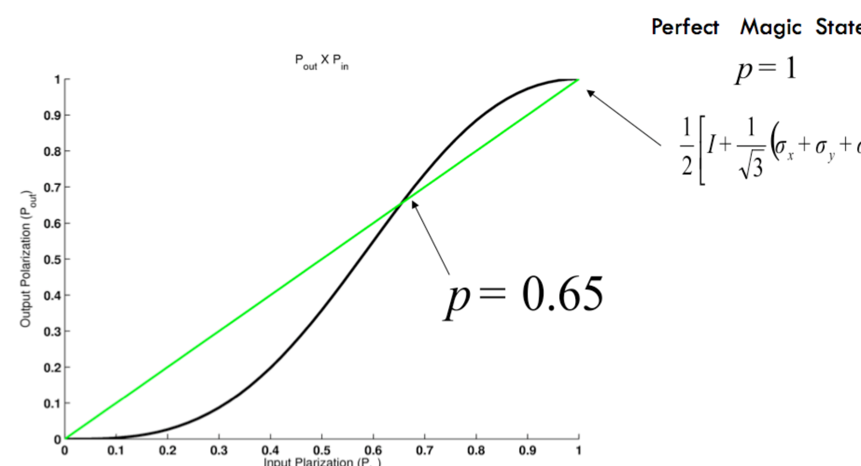

Magic state distillation

Use crotonic acid

	M	H_1	H_2	C_1	C_2	C_3	C_4	Spin	T_2(s)
M	-1309							M	0.84
H_1	6.9	-4864						H_1	0.85
H_2	-1.7	15.5	-4086					H_2	0.84
C_1	127.5	3.8	6.2	-2990				C_1	1.27
C_2	-7.1	156.0	-0.7	41.6	-25488			C_2	1.17
C_3	6.6	-1.8	162.9	1.6	69.7	-21586		C_3	1.19
C_4	-0.9	6.5	3.3	7.1	1.4	72.4	-29398	C_4	1.13

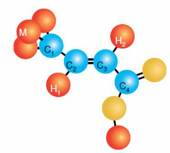

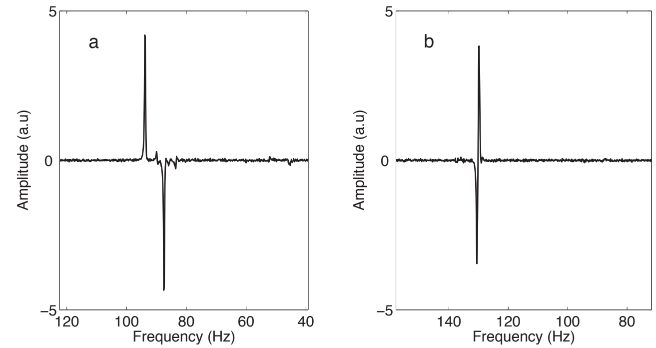

Distill and get (for the 5 qubits)

$$\theta_1\rho_1|00000\rangle\langle 00000| + \theta_2\rho_2|00001\rangle\langle 00001| + \ldots$$

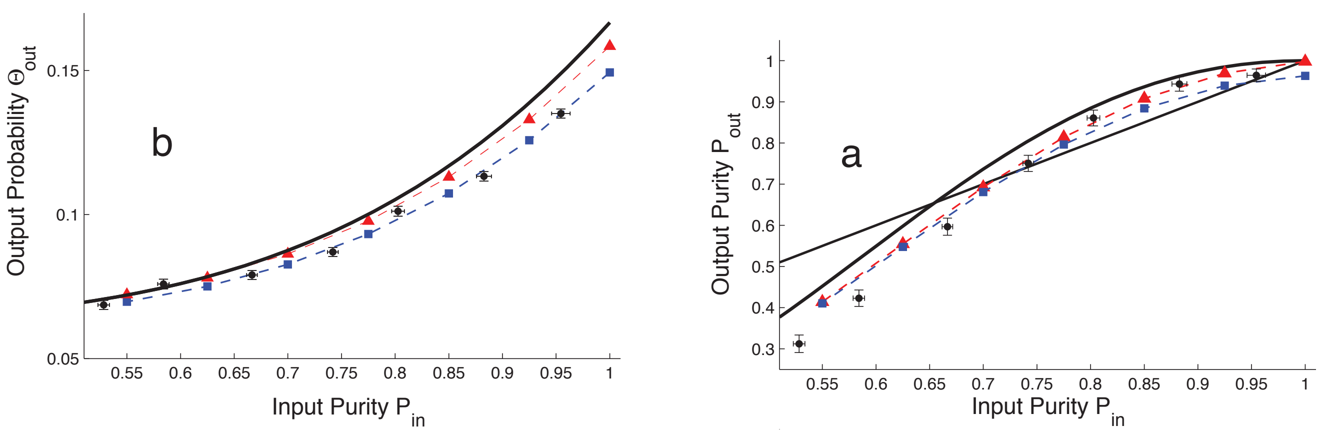

Input	Output
0.95	0.96
0.88	0.94
0.80	0.86
0.73	0.74
0.67	0.59

A. M. Souza, J. Zhang, C.A. Ryan1 & R. Laflamme; Nature Communications, 2;169, 2011

Conclusion

In order to implement quantum error correction, we need

- **Good knowledge of the noise**
- **Good quantum control**
- **Ability to extract entropy**
- **Parallel operations**

We have seen, in the last 4 years, an increased integration of these requirements, much better control, and operations on a larger number of qubits.

But it is only the beginning of experimental QEC and its fault tolerant implementations.

Thanks to Pdfs and Students

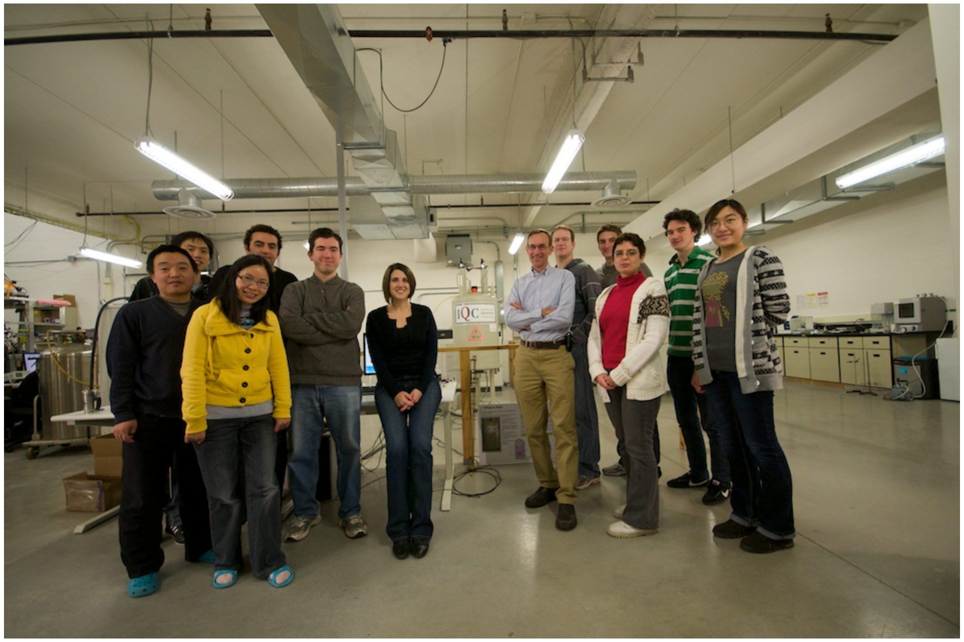

Jingfu Zhang
Urbasi Sinha
Osama Moussa
Robabeh Rahimi
Gina Passante
Guanru Feng
Ben Criger
Daniel Park
Chris Erven
Xian Ma
Tomas Jochym-O'Connor
Joseph Rebstock

Alumni group members

Colm Ryan
Martin Laforest
Alexandre deSouza
Jeremy Chamilliard
Jonathan Baugh
Marcus Silva
Camille Negrevergne
Casey Myers

Thanks

Ontario

ACTION PLAN PLAN D'ACTION

Industry Canada Industrie Canada

Canada

Canada Foundation for Innovation
Fondation canadienne pour l'innovation

NSERC
CRSNG

COM DEV

INO

IBM

I A R P A
BE THE FUTURE

RIM

NIST

Canadian Space Agency	Agence Spatiale Canadienne
Defence Research and Development Canada	Recherche et developpement pour la defense Canada
Canada Research Chairs	Chaires de recherche du Canada
Human Resources and Social Development Canada	Ressources humaines et Développement social Canada
Communications Security Establishment Canada	Centre de la securite des telecommunications Canada